Mon. Not. R. Astron. Soc. **363,** 763–768 (2005) doi:10.1111/j.1365-2966.2005.09589.x

Photospheric phosphorus in the *FUSE* spectra of GD71 and two similar DA white dwarfs

P. D. Dobbie,[1⋆] M. A. Barstow,[1] I. Hubeny,[2] J. B. Holberg,[3] M. R. Burleigh[1] and A. E. Forbes[1]

[1]*Department of Physics and Astronomy, University of Leicester, University Road, Leicester LE1 7RH*
[2]*Department of Astronomy and Steward Observatory, University of Arizona, Tucson, AZ 85721, USA*
[3]*Lunar and Planetary Laboratory, Gould-Simpson Building, University of Arizona, Tucson, AZ 85721, USA*

Accepted 2005 July 27. Received 2005 July 27; in original form 2005 July 15

ABSTRACT

We report the detection, from the *Far Ultraviolet Spectroscopic Explorer (FUSE)* data, of phosphorus in the atmospheres of GD71 and two similar DA white dwarfs. This is the first detection of a trace metal in the photosphere of the spectrophotometric standard star GD71. Collectively, these objects represent the coolest DA white dwarfs in which photospheric phosphorus has been observed. We use a grid of homogeneous non-local thermodynamic equilibrium synthetic spectra to measure abundances of $[\mathrm{P/H}] = -8.57^{+0.09}_{-0.13}$, $-8.70^{+0.23}_{-0.37}$ and $-8.36^{+0.14}_{-0.19}$ in GD71, RE J1918+595 and RE J0605−482 respectively. At the observed level we find that phosphorus has no significant impact on the overall energy distribution of GD71. We explore possible mechanisms responsible for the presence of this element in these stars, concluding that the most likely is an interplay between radiative levitation and gravitational settling, possibly modified by weak mass loss.

Key words: stars: abundances – stars: individual: GD71 – white dwarfs.

1 INTRODUCTION

The compositions of the atmospheres of white dwarfs are observed to be dominated by the lightest elements, H (DAs) or He (DO/DBs), as predicted several decades ago by theory (Schatzman 1958). Unimpeded, the high surface gravities of these objects cause heavier elements to settle out on time-scales of mere days (e.g. Dupuis et al. 1993). Nevertheless, ultraviolet observations have revealed trace quantities of metals in the photospheres of a large number of hot white dwarfs ($T_{\rm eff} \gtrsim 40\,000$ K), e.g. C, Fe and Ni in G191-B2B (Bruhweiler & Kondo 1983; Vennes et al. 1992; Holberg et al. 1994) and a handful of cooler degenerates e.g. Si in Wolf 1346 ($T_{\rm eff} \approx 20\,000$ K; Holberg et al. 1996). Furthermore, high-resolution optical spectroscopic observations have shown that ∼20 per cent of DAs cooler than 10 000 K are DAZ stars, that is they contain observable quantities of Ca, Mg, and Fe (Zuckerman et al. 2003). Clearly, there are processes operating in the photospheres of these objects which can compete against gravitational settling.

Several theoretical studies have shown that the transfer of net upward momentum from the intense radiation field to heavy elements via their bound–bound transitions can prevent small but detectable quantities of metals from sinking out of the photospheres of white dwarfs with $T_{\rm eff} \gtrsim 20\,000$ K (e.g. Vauclair, Vauclair & Greenstein 1979). A number of these investigations have made relatively precise predictions regarding the abundances of heavy elements as a function of surface gravity and effective temperature (e.g. Chayer et al. 1995a; Schuh 2005). Indeed, these calculations are able to qualitatively reproduce some of the more general trends, affirming radiative levitation as an influential mechanism in preventing gravitational settling in the atmospheres of these hotter stars. For example, they successfully replicate the observed sharp decline in the abundance of Fe at $T_{\rm eff} \approx 50\,000$ K and the observed decrease with $T_{\rm eff}$ in the overall metal content of white dwarf photospheres. Further, in accord with these calculations the abundances of elements such as C and N appear to be largely independent of effective temperature at $T_{\rm eff} \gtrsim 50\,000$ K (see Barstow et al. 2003a).

However, at a more quantitative level, there are significant discrepancies between observed heavy element abundances and the predictions of equilibrium radiative levitation theory. On theoretical grounds, stars with comparable effective temperatures and surface gravities are expected to have similar photospheric abundances, but in reality can show radically different compositions. For example, while the observed energy distribution of GD153 is consistent with that of a pure-H atmosphere, GD394 and RE1614−085 contain significant quantities of silicon ($[\mathrm{Si/H}] = -5.1 \pm 0.1$) and nitrogen ($[\mathrm{N/H}] = -3.6 \pm 0.1$) respectively, despite all three objects having $T_{\rm eff} \approx 38\,000$ K and $\log g \approx 7.8$ (Holberg et al. 1997). It has often been argued that these anomalies indicate other processes

⋆E-mail: pdd@star.le.ac.uk

(e.g. accretion or mass loss) that act in conjunction with radiative levitation, at least in some stars, to dictate photospheric composition.

Our survey of the abundances of C, N, O, Si, Fe and Ni in the photospheres of 25 hot DA white dwarfs is the most comprehensive undertaken to date, and has unearthed a number of interesting results (see Barstow et al. 2003). However, it was based largely on *Hubble Space Telescope (HST)* Space Telescope Imaging Spectrograph data, a sample that cannot now be enlarged due to instrument failure. To gain a more complete understanding of the relative influence of each of these physical processes it is important to continue enlarging the sample of stars for which robust measurements and limits on the abundances of photospheric metals are available. Further, it is particularly important to increase the number of such stars in effective temperature ranges where few objects have previously been studied (e.g. $20\,000\,\mathrm{K} \lesssim T_{\rm eff} \lesssim 40\,000\,\mathrm{K}$). Over the last few years the *Far Ultraviolet Spectroscopic Explorer (FUSE)* has observed a large number of white dwarfs. This has led to the provision of a collection of homogeneous spectroscopic data covering $\lambda \approx$ 900–1200 Å , with generally a moderate-to-good signal-to-noise ratio (S/N), for $\gtrsim$100 DAs. Much of this data is now in the public domain and available for download from the Multimission Archive at Space Telescope (MAST). These *FUSE* observations offer the benefit, over *IUE* and *HST* data, of access to resonance lines of P and S. Thus photospheric abundance surveys can now be expanded to include these two additional elements.

GD71 (WD0459+158), first catalogued by Giclas, Burnham & Thomas (1965), is a bright nearby hot DA white dwarf lying virtually in the middle of the aforementioned temperature range ($T_{\rm eff} \approx 32\,000$ K). It has been studied extensively at optical, UV, EUV and near-IR wavelengths and is widely used as a photometric and spectrophotometric calibration star (e.g. Landolt 1992; Bohlin, Dickensen & Calzetti 2001). Within their respective statistical uncertainties, the *International Ultraviolet Explorer (IUE)* and *Extreme Ultraviolet Explorer (EUVE)* spectra of GD71 are entirely consistent with a pure-H atmosphere and to date no heavy elements have been detected in its photosphere (Barstow et al. 1997; Holberg, Barstow & Sion 1998). Indeed, for spectrophotometric calibration purposes it has been assumed to have a pure-H composition (e.g. Bohlin 1996). However, we have chosen to examine this assumption more closely, since (1) radiative levitation theory predicts the presence of small but nevertheless detectable quantities of photospheric metals down to $T_{\rm eff} \approx 20\,000$ K (e.g. Si, Al and P); (2) to date only a handful of objects have been studied in detail in the range $20\,000\,\mathrm{K} \lesssim T_{\rm eff} \lesssim 40\,000$ K; and (3) there exists a *FUSE* spectrum with good S/N ($\sim$30) for this white dwarf.

In the current work we present an analysis of the *FUSE* spectrum of GD71. We identify a number of spectral features attributable to the interstellar medium. In addition, we detect high-ionization P features, and argue that they arise in the stellar photosphere. We use a grid of non-local thermodynamic equilibrium (LTE) model atmospheres to determine [P/H]. Finally, we discuss our findings in the context of radiative levitation theory and the processes of accretion and mass loss.

2 OBSERVATIONS

2.1 A *FUSE* observation of GD71

An observation of GD71 was obtained with *FUSE* operating in time-tag (TTAG) mode and in the LWRS configuration on 2000/11/04. We have acquired the relevant raw data products from the Multimission Archive at the Space Telescope Science Institute (MAST). A summary of this observation is presented in Table 1.

Table 1. The log of the *FUSE* observation of GD71.

Observation ID	Aperture/mode	Start date	Exp. time (s)
P2041701000	LWRS/TTAG	2000 Nov 04	13928

Several detailed descriptions of the*FUSE* instrumentation already exist in the literature (e.g. Green, Wilkinson & Friedman 1994), so we only give a brief description of the features most relevant to the current analysis. The spectrometer consists of four separate optical channels. To maximize the throughput, it is important that all four are properly illuminated by the target. However, it has proved difficult to maintain optimal alignment for the duration of an observation due to in-orbit movement in the mirrors and gratings. Consequently, most observations have been obtained through the large square aperture ($30 \times 30\,\mathrm{arcsec}^2$) of the LWRS configuration which limits the spectral resolution to between $R = 10\,000$–$20\,000$.

We have processed the raw data with a recent version of CALFUSE (v3.0). The pipeline procedure nominally flux- and wavelength-calibrates the data, correcting for geometric distortions and flagging as low-quality data obtained on dead spot areas of the detectors. However, this version of the software does not correct for the impact on the count rates of the 'worm', a strip of flux attenuated by up to 50 per cent, running in the dispersion direction of the spectra. An inspection of the count rate plots for each channel produced by the pipeline suggests that GD71 remained comfortably within the LWRS apertures throughout the duration of this observation. Furthermore, an examination of the individual extracted 1D spectra indicates that the 'worm' only affected data from the LiF 1b detector segment significantly.

Prior to coadding the individual data sets to obtain a single far-ultraviolet (FUV) spectrum of GD71 with optimal S/N, it was necessary to account for drifts in the wavelength scale between the subintegrations of the observation. The exposures for each segment were cross-correlated by running the IDL routine CROSS_CORRELATE on the regions which included the most distinct absorption features (e.g. the N I triplet at 1134 Å for LiF 1b and LiF 2a). Small wavelength corrections were calculated and applied to the data. The alignments of the exposures for each segment were examined by eye, and, where improvement was necessary or possible (e.g. where geocoronal emission had impacted on the results of the CROSS_CORRELATE algorithm), further small shifts were applied manually to their wavelength scales. A co-added data set for each segment was then produced where each subintegration was weighted according to exposure time. Any data found to be significantly affected by the worm were discarded. As they generally have the lowest S/N and the poorest wavelength solution, data from the edges of each spectrum were also rejected. Sections of these data sets which include strong absorption lines were cross-correlated and any linear wavelength shifts with respect to the LiF 1a segment were calculated and applied to each spectrum. However, the *FUSE* spectrum of GD71 contains no strong absorption features in the ranges 995–1010 and 1090–1110 Å. Therefore the measured wavelengths of sharp line features arising from species H I, C II, O I, and N I, which were assumed to have a common interstellar origin, were used to apply a fine adjustment to the wavelength scales of the SiC 1b, SiC 2a, LiF 1b and LiF 2a segments. Finally, the spectra were resampled on to a single wavelength scale with 0.04-Å binning, and were co-added, weighting each by the inverse of the statistical variance of the data determined over intervals of 20 Å.

2.2 Absorption features in the co-added FUV spectrum of GD71

The co-added *FUSE* spectrum has been run through a series of custom-written scripts to:

(i) normalize the data;
(ii) flag probable absorption features;
(iii) fit Gaussians or, where appropriate, multiple Gaussians to determine central wavelengths and equivalent widths of features; and
(iv) assign each feature a likely identification based on the measured radial velocity and the ionization state of the proposed progenitor species.

The results of this process are summarized in Table 2. We note that the 1σ errors in central wavelengths, derived from a χ^2 fitting process, underestimate the true uncertainties as illustrated by the scatter in the velocity measurements. We believe this discrepancy is a result mainly of residual uncertainties in the *FUSE* pipeline wavelength calibration and small imperfections in our alignment of the spectral segments.

Holberg et al. (1998) reported the detection of interstellar O I (1302.169 Å) and Si II (1190.416,1260.442 Å) in the *IUE* echelle spectrum of GD71 and determined a weighted mean velocity of $+23.2 \pm 2.5$ km s^{-1} for these features. Based on observations of objects with independently determined radial velocities, the absolute wavelength scale of *IUE* echelle data processed with NEWSIPS is found to be accurate to 3–5 km s^{-1} (Holberg et al. 1998). The nominal absolute calibration of the *FUSE* wavelength scale is considered to be limited to $\sim$15 km s^{-1} by uncertainty in the position of the target within the LWRS aperture (e.g. Oegerle et al. 2005). We have determined a weighted mean velocity of -0.3 ± 0.6 km s^{-1} for the low ionization lines of C II (1036.337 Å) and O I (1039.230 Å) which lie within the wavelength range covered by the LiF 1a segment (987.1–1082.3 Å) and almost certainly have the same origin as the lines reported by Holberg et al. Since these results indicate an offset in the *FUSE* data of ≈ -20 km s^{-1} with respect to the more robust wavelength scale of the *IUE* echelle spectrum, in subsequent discussions we apply a systematic shift of $+23.5 \pm 2.6$ km s^{-1} to the velocities determined from the *FUSE* data.

Unfortunately, high-resolution spectroscopic measurements of the core of the Hα line formed in the atmosphere of GD71 indicate that the stellar photosphere has a similar velocity (e.g. the weighted mean of the measurements of Maxted, Marsh & Moran 2000 is $+30.0 \pm 1.5$ km s^{-1}) to the interstellar medium (ISM) along this line of sight ($+23.2 \pm 5.6$ km s^{-1} allowing for a potential uncertainty of 5 km s^{-1} in the absolute calibration of the *IUE* echelle data). Thus radial velocities alone do not constitute a suitable indicator by which to distinguish between a photospheric and an interstellar origin for absorption features detected in this particular *FUSE* data set. Nevertheless, when the comparatively high effective temperature of GD71, the low ionization states of the progenitor species and previously published results based on *FUSE* observations of DA white dwarfs (e.g. Lehner et al. 2003) are taken into account, the vast majority of lines listed in Table 2 can be attributed to the ISM.

Table 2. Summary details of the main absorption features identified in the co-added *FUSE* spectrum of the white dwarf GD71.

Ion	Lab	Obs	v	Δv	EW	ΔEW
	Å		km s^{-1}		mÅ	
			Interstellar			
H I	917.181	917.196	4.9	4.9	168	19
H I	918.129	918.130	0.3	4.1	135	16
H I	919.351	919.356	1.6	4.9	156	11
H I	920.963	920.959	−1.3	4.6	180	11
H I	923.150	923.152	0.6	8.3	194	12
H I	926.226	926.234	2.6	2.3	175	14
H I	930.748	930.728	−6.4	1.3	161	14
H I	937.803	937.780	−7.4	1.0	151	13
H I	949.743	949.747	1.3	1.3	175	13
O I	976.448	976.421	−8.3	1.5	10	4
C III	977.020	977.013	−2.1	1.5	41	6
N III†	989.799	989.838	11.8	3.9	31	4
Si II†	989.873	989.838	−10.6	3.9	31	4
C II	1036.337	1036.334	−0.9	0.6	56	2
O I	1039.230	1039.242	3.5	1.5	11	2
N II	1083.990	1084.016	7.2	1.0	28	4
N I††	1134.165	1134.155	−2.6	5.7	4	2
N I††	1134.415	1134.426	2.9	1.8	17	3
N I††	1134.980	1134.997	4.5	1.2	15	2
Fe II	1144.938	1144.948	2.6	3.7	4	2
			Photospheric			
P III	1003.600	1003.615	4.5	5.1	5	2
P V	1117.977	1117.985	2.1	2.8	13	3
P V	1128.008	1128.020	3.2	1.7	4	2

†Blended ?
††Some contamination from N I geocoronal emission.

2.3 High ionization phosphorus lines in the *FUSE* spectrum of GD71

A closer inspection of the co-added *FUSE* spectrum has also revealed several weak features arising from species of relatively high ionization states, e.g. the resonance lines of P V at 1117.977 and 1128.008 Å. The velocities of these transitions are identical within the measurement uncertainties so they probably have a common origin (see Table 2). Although these lines are coincident in velocity space with a number of features attributable to the ISM, residual uncertainties in the wavelength calibration of this data set and the similarity between the velocities of the ISM along this line of sight and the atmosphere of GD71, as discussed above, mean that an interstellar, circumstellar or photospheric origin cannot be ruled out at this stage. Nevertheless, other considerations indicate the former interpretation is unlikely. For example, the ionization stages of the progenitor ions are higher than those typically found in the ISM. The P III 1003.600-Å line arises from the $2P^o$-2S multiplet and has a lower level 0.07 eV above the ground state. Furthermore, in a solar mixture P is less abundant by a factor 1000 than C, N or O.

To examine the two other possible origins in more detail, we have acquired from MAST the *FUSE* data products for two further white dwarfs with effective temperatures and surface gravities similar to those of GD71. Vennes et al. (1997) derive $T_{\rm eff} = 33\,000$ K, $\log g = 7.90$ for REJ1918+595, while Marsh et al. (1997), Finley, Koester & Basri (1997) and Vennes et al. (1997) derive $T_{\rm eff} = 33\,040$ K, $\log g = 7.80, T_{\rm eff} = 35\,332$ K, $\log g = 7.84$ and $T_{\rm eff} = 35\,600$ K, $\log g = 7.76$ respectively for RE J0605−482. FUV observations of RE J1918+595 and RE J0605−482, in TTAG mode and in the LWRS configuration, were obtained on 2002 May 7 and 2002 December 31, respectively.

For each of these two stars we have constructed a co-aligned and co-added the *FUSE* spectrum in the manner described above. In each data set we have determined the velocities of features attributable to the ISM, e.g. N I (1134.165, 1134.415, 1134.980 Å), Fe II (1144.938 Å) and the stellar photosphere e.g. Si III (1108.368, 1109.957, 1113.219 Å) and Si IV (1122.485, 1128.340 Å), where

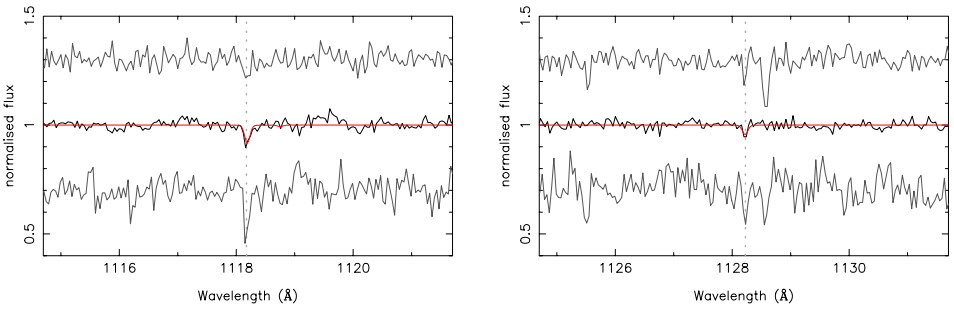

Figure 1. Sections of the normalized *FUSE* spectra of REJ1917+599 (top), GD71 (middle) and REJ0605−482 (bottom) showing the resonance lines of P V (1117.977,1128.008 Å) which we attribute to the stellar photospheres. Photospheric Si IV (1128.334-Å) and interstellar Fe II (1125.448-Å) lines are also seen in the top and bottom data sets. The best-fitting model representation of the GD71 data is overplotted (red).

the rest wavelengths of the Si lines are determined from the predictions of appropriate non-LTE model atmospheres. The weighted mean velocities of these interstellar and photospheric lines in the spectrum of RE J1918+595 are $+23.5 \pm 0.3$ km s^{-1} and $+59.8 \pm 0.9$ km s^{-1} respectively. In the spectrum of RE J0605−482, these features have weighted mean velocities of $+18.2 \pm 0.7$ km s^{-1} and $+53.1 \pm 2.8$ km s^{-1} respectively. Thus in the spectra of these two objects, the ISM and the photosphere have quite distinct velocities.

Scrutiny of the data for RE J1918+595 and RE J0605−482 reveals the presence of P V resonance lines, at weighted mean velocities of $+55.3 \pm 1.5$ km s^{-1} and $+53.7 \pm 0.6$ km s^{-1} respectively. A previous high-resolution UV study has revealed circumstellar features along the lines of sight to nine out of a sample of 23 hot DA white dwarfs (Bannister et al. 2003). In the vast majority of these nine cases the difference in the velocities of the circumstellar and interstellar features was found to be less than 10 km s^{-1}. The difference in velocity between the P V transitions and the ISM lines in the *FUSE* spectra of RE J1918+595 and RE J0605−482 are 31.8 ± 1.5 km s^{-1} and 35.5 ± 3.0 km s^{-1} respectively, arguing against a circumstellar origin. Indeed, given the scatter typically seen in our measurements, the velocities of the P V lines strongly support a photospheric interpretation. In Fig. 1 we show sections of the *FUSE* spectra of GD71, RE J1918+595 and RE J0605−482 centred on the P V resonance transitions. For the purposes of this plot we have applied a shift to the wavelength scales to co-align the 1117.977-Å line in the three data sets.

On the weight of the above evidence, we conclude that the most likely origin of the high ionization P lines identified in the *FUSE* spectrum of GD71 is the stellar photosphere. Accepting this, we now use model atmosphere calculations to place constraints on the abundance of photospheric phosphorus in these three DAs.

3 THE MODEL ATMOSPHERE CALCULATIONS

The models utilized in this work have been generated with the latest versions of the plane-parallel, hydrostatic, non-LTE atmosphere and spectral synthesis codes TLUSTY (v200; Hubeny 1988; Hubeny & Lanz 1995; Hubeny & Lanz, private communication) and SYNSPEC (v48; Hubeny et al. 1994a). We have employed state-of-the-art model ions of H and P. The H I ion incorporates the eight lowest energy levels and one superlevel extending from $n = 9$ to $n = 80$, where the dissolution of the high-lying levels was treated by means of the occupation probability formalism of Hummer & Mihalas (1988), generalized to the non-LTE situation by Hubeny, Hummer & Lanz (1994b). The P IV and P V model ions were developed by Lanz & Hubeny (2003) for the study of O-stars and full details may be found therein. The P III ion, which incorporates the nine lowest levels, was constructed in a similar manner, except the online version of AUTOSTRUCTURE[1] was used to estimate oscillator strengths where experimental values were unavailable. All calculations were carried out under the assumption of radiative equilibrium and incorporated a full treatment of line-blanketing effects. During the calculation of the model structure, the lines of the Lyman and Balmer series were treated by means of an approximate Stark profile; in the spectral synthesis step, detailed profiles for the Lyman lines were calculated from the Stark broadening tables of Lemke (1997).

Table 3. Results of homogeneous model fitting procedure.

Star	$T_{\rm eff}$	$\log g$	[P/H]
GD71	32625^{+15}_{-25}	$7.89^{+0.01}_{-0.01}$	$-8.57^{+0.09}_{-0.13}$
RE J1918+595	32030^{+95}_{-95}	$7.79^{+0.03}_{-0.04}$	$-8.70^{+0.23}_{-0.37}$
RE J0605−482	34370^{+190}_{-175}	$7.79^{+0.06}_{-0.05}$	$-8.36^{+0.14}_{-0.19}$

Numerous estimates of the effective temperature and surface gravity of GD71 are available in the literature e.g. Marsh et al. (1997), Finley et al. (1997) and Vennes et al. (1997) derive $T_{\rm eff} = 32\,008$ K, $\log g = 7.70$, $T_{\rm eff} = 32\,747$ K, $\log g = 7.68$ and $T_{\rm eff} = 33\,000$ K, $\log g = 7.88$ respectively by fitting synthetic profiles to the observed Balmer lines. Hence we generated a grid of H+P models spanning the ranges $T_{\rm eff} = 30\,000$–$35\,000(2500)$ K, $\log g = 7.5$–$8.5(0.5)$ and [P/H] = −12–−7.0(1.0). Our general spectral analysis techniques have been described at length in previous publications. so only aspects specific to the current work are detailed here. For computational speed, only those regions of the co-added, optimal S/N data set that include the Lyman lines and the locations of the phosphorus transitions predicted to be most prominent in this effective temperature and surface gravity range were incorporated into the spectral fitting process (e.g. 930-990 Å, 1000–1050 Å, 1116–1120 Å and 1126–1130 Å). During the analysis, each of these sections was assigned an independent normalization parameter to circumvent any residual errors in the shape of the continuum flux. All errors quoted here are 1σ unless stated otherwise, but as these are derived formally from the fitting process, they may underestimate the true uncertainties. The parameters of our best-fitting homogeneous model representations of the *FUSE* spectra of all three white dwarfs are given in Table 3. We note that the energy distribution of the GD71 model is indistinguishable from that of a pure-H composition from 10–10 000 Å, except in a few narrow regions which include P lines.

[1] http://random.ivic.ve/autos/

4 DISCUSSION

4.1 Photospheric phosphorus in DA white dwarfs

Bruhweiler (1984) reported the possible detection of N V, C IV and Si IV resonance lines in a single *IUE* spectrum of GD71 but concluded that these were most likely formed in a halo region around the star. A subsequent examination of a co-added data set derived from the three existing *IUE* echelle spectra failed to confirm the existence of these features at the 30 mÅ equivalent width level and instead detected only the strong resonance lines of interstellar O I and Si II (Holberg et al. 1998). Hence the current work represents the first probable detection of a heavy element in the atmosphere of the flux standard star GD71.

Phosphorus was first revealed in the atmospheres of the hot DA white dwarfs G191-B2B and MCT0455−2812 by the *Orbiting and Retrievable Far and Extreme Ultraviolet Spectrometer (ORFEUS)* observations (Vennes et al. 1996). Subsequently, photospheric phosphorus has been reported in the *FUSE* spectra of a significant number of other hot ($T_{\rm eff} \gtrsim 40\,000$ K) hydrogen-rich degenerates (e.g. GD246, Feige 55, Wolff et al. 2001 and RE1032+532, Dupuis et al. 2004). However, to date, phosphorus has been detected in the atmospheres of only two DAs with $T_{\rm eff} < 40\,000$ K, GD394 ($T_{\rm eff} \approx 39\,500$ K; Chayer et al. 2000) and GD659 ($T_{\rm eff} \approx 36\,000$ K; Dupuis et al. 2004). The white dwarfs analysed in this paper, therefore, represent the three coolest DAs in which photospheric phosphorus has yet been found.

4.2 Possible mechanisms for photospheric phosphorus in these white dwarfs

While the presence of a close cool companion can lead, through accretion of wind material, to heavy-element contamination in a white dwarf atmosphere (e.g. V471 Tauri; Sion et al. 1998) it seems rather unlikely that this is the source of the phosphorus observed in these stars. For example, Maxted et al. (2000) find no evidence of radial velocity variations in GD71, while Dobbie et al. (2005) have used near-IR spectroscopy to set a limit of $M < 0.072\,{\rm M}_{\odot}$ on the mass of any such companion. Furthermore, 2MASS data provide no evidence of a near-IR excess to either REJ1917+488 or REJ0605−482 (e.g. Skrutskie et al. 1997). While the presence of a close substellar companion to any of these stars cannot be excluded, recent work by Farihi, Becklin & Zuckerman (2005) argues against this.

Alternatively, equilibrium radiative levitation calculations indicate that observable quantities of phosphorus should be supported in the photospheres of typical DA white dwarfs to $T_{\rm eff} \approx 32\,500$ K (Vennes et al. 1996). Indeed, the phosphorus abundances we measure for these three stars seem to be satisfyingly consistent with the theoretical values (see Vennes et al.'s fig. 4). At face value, the lowest and largest abundance is measured in the coolest and hottest star respectively. However, the results of a preliminary study of the *FUSE* spectra of 28 hot DA white dwarfs indicate that this agreement might be simply fortuitous. In many objects with $35\,000\,{\rm K} \lesssim T_{\rm eff} \lesssim 55\,000$ K, phosphorus is found to be underabundant, often strongly, with respect to the predictions (Dupuis et al. 2004). The abundance of an element, in equilibrium, is generally depth-dependent (e.g. Schuh 2005). The predictions of Vennes et al. (1996) correspond to the phosphorus abundance at the Rosseland photosphere ($\tau_{\rm Ross} \approx 2/3$), which may differ significantly from that in the line-formation region from which the observed abundances are determined. Therefore, to appraise the rôle of radiative levitation in more detail we have constructed a small number of fully self-consistent H+P model atmospheres. In these calculations we have used information on the ionization fraction of phosphorus and on the detailed radiation field gleaned from SYNSPEC to determine the effective gravitational downward forces and the upward radiative forces on phosphorus ions as a function of depth in the atmosphere. An estimate of the phosphorus abundance at each depth point has been obtained by equating these forces (e.g. Chayer et al. 1995b). The estimates have been fed back into TLUSTY and an updated model structure determined. The entire process has been repeated until the abundances converge to $\lesssim$3 per cent throughout most of the atmosphere. In the uppermost layers this restriction has been relaxed to $\lesssim$10 per cent but has no significant impact on the emergent spectrum.

The results of these calculations consolidate previous predictions that detectable levels of phosphorus remain supported in the atmospheres of typical DA white dwarfs at the effective temperatures examined here. However, the metal absorption lines predicted by our non-LTE models are considerably stronger than those observed in the *FUSE* data. For example, if we attempt to fit our homogeneous grid to the emergent spectra from the self-consistent calculations with effective temperatures and surface gravities appropriate to RE J1918+595 and GD71, we derive [P/H] ≈ -7.3. If instead we fit the self-consistent models to the observed phosphorus features only, fixing the effective temperature at the values determined in Section 3, we find the element abundance profile appropriate to $\log g = 8.43$, 8.44 and 8.45 provides the best representation of these data, for RE J0605−482, GD71 and RE J1918+595 respectively. These gravities are greater by ∼0.6 dex than those estimated from the Lyman line series. The apparent discrepancy between the results from our modelling and the predictions of Vennes et al. (1996) likely stems from the abundance of phosphorus at the Rosseland photosphere, $\log_{10}$ (model column mass depth) ~ -2, decreasing rapidly with effective temperature at $T_{\rm eff} \lesssim 35\,000$ K, while in the P line-forming region, $\log_{10}$ (model column mass depth) ~ -3.5, maintaining a greater value.

Interestingly, in their analysis of the *EUVE* spectra of 26 DA white dwarfs ($T_{\rm eff} \gtrsim 40\,000$ K) in which a grid of self-consistent stratified models was compared by eye to the data, in effect allowing effective temperature and surface gravity to vary freely, Schuh, Dreizler & Wolff (2002) found, more often than not, that the calculation which best represented the observed energy distribution of a white dwarf had a larger surface gravity (∼0.4 dex) than the value determined for the star via Balmer line fitting. Schuh (2005) has estimated that the complexities in accurately calculating the radiative force on an element in a stellar photosphere, e.g. due to the opacities of other metals, can result in uncertainties of up to 2 dex in the abundances derived at some depth points in their calculations. We note that the three white dwarfs analysed here are more metal-poor and somewhat cooler than those typical of her sample, lying in a range where non-LTE models replicate the structure of the stellar photosphere more satisfactorily (Barstow et al. 2003b). Indeed, test calculations reveal that the inclusion of additional metals, e.g. C and Si, has no significant impact on the P abundance profile. However, robust and comprehensive atomic data for P are not available from the TOPBASE database (Cunto & Mendoza 1992), so shortcomings in the current model ions and line lists for this element may counter any advantage here.

Of course the balance between radiative levitation and gravitational settling can be disturbed by mass loss. From a series of exploratory time-dependent calculations involving Si, that authors Chayer, Fontaine & Pelletier (1997) find that at moderate mass-loss rates ($10^{-16} \lesssim \dot{M} \lesssim 10^{-14}\,{\rm M}_{\odot}\,{\rm yr}^{-1}$), the reservoir of this element is exhausted after a few $\times\ 10^4$ yr, after which it is depleted rapidly

from the stellar photosphere (few $\times 10^5$ yr) to levels well below the detection threshold of the *FUSE* data. At very low rates of mass loss (e.g. $\dot{M} \lesssim 10^{-18}\,M_\odot\,yr^{-1}$), the Si abundance profile is essentially that predicted by equilibrium radiative levitation theory up to the end of their calculations. The mere detection of phosphorus in these three stars would appear to argue against mass loss at the larger rates discussed above. Nevertheless, it seems plausible that this process may be operating at low levels in these stars and that it is the slow exhaustion of an underlying reservoir of this element which results in observed abundances below the equilibrium radiative levitation prediction.

ACKNOWLEDGMENTS

PDD and MBU are supported by PPARC. JBH wishes to acknowledge support from NASA ADP grant NNG05GC46G. Based on observations made with the NASA-CNES-CSA *Far Ultraviolet Spectrscopic Explorer. FUSE* is operated for NASA by the Johns Hopkins University under NASA contract No. NAS5-32985. We express our thanks to the anonymous referee for a very prompt and useful report.

REFERENCES

Barstow M. A., Dobbie P. D., Holberg J. B., Hubeny I., Lanz T., 1997, MNRAS, 286, 58
Barstow M. A., Good S. A., Holberg J. B., Hubeny I., Bannister N. P., Bruhweiler F. C., Burleigh M. R., Napiwotzki R., 2003a, MNRAS, 341, 870
Barstow M. A., Good S. A., Burleigh M. R., Hubeny I., Holberg J. B., Levan A. J., 2003b, MNRAS, 344, 562
Bannister N. C., Barstow M. A., Holberg J. B., Bruhweiler F. C., 2003, MNRAS, 341, 477
Bohlin R. C., 1996, AJ, 111, 1743
Bohlin R. C., Dickensen M. E., Calzetti D., 2001, AJ, 122, 2118
Bruhweiler F. C., 1984, in Mead J. M., Kondo Y., Chapman R., eds, Future of UV astronomy based on six years of IUE Research. NASA, CP-2349, p. 269
Bruhweiler F. C., Kondo Y., 1983, ApJ, 269, 657
Chayer P., Vennes S., Pradhan A. K., Thejll P., Beauchamp A., Fontaine G., Wesemael F., 1995a, ApJ, 454, 429
Chayer P., Fontaine G., Wesemael F., 1995b, ApJS, 99, 189
Chayer P., Fontaine G., Pelletier C., 1997, in Isern J., Hernanz M., Garcia-Berro E., eds, Astrophys. and Space Sci. Library Vol. 214, Proc. 10th European Workshop on White Dwarfs. Kluwer, Dordrecht, p. 253
Chayer P., Kruk J. W., Ake T. B., Dupree A. K., Malina R. F., Siegmund O. H. W., Sonneborn G., Ohl R. G., 2000, ApJ, 538, L91
Cunto W., Mendoza C., 1992, Rev. Mex. Astron. Astrofis., 23, 107
Dobbie P. D., Burleigh M. R., Levan A. J., Barstow M. A., Napiwotzki R., Holberg J. B., Hubeny I., Howell S. B., 2005, MNRAS, 357, 1049
Dupuis J., Fontaine G., Pelletier C., Wesemael F., 1993, ApJS, 84, 73
Dupuis J., Chayer P., Kruk J. W., Vennes S., 2004, in de Martino D., Silvotti R., Solheim J.-E., Kalytis R., eds, NATO Science Series II - Mathematics, Physics and Chemistry Vol. 105, White Dwarfs. Kluwer Academic, Dordrecht, p. 157
Farihi J., Becklin E. E., Zuckerman B., 2005, ApJS, accepted (astro-ph/0506017)
Finley D. S., Koester D., Basri G., 1997, ApJ, 488, 375
Giclas H. L., Burnham R., Thomas N. G., 1965, Lowell Observatory Bulletin No. 125, p. 155
Green J. C., Wilkinson E., Friedman S. D., 1994, Proc. SPIE, 2283, 12
Holberg J. B., Hubeny I., Barstow M. A., Lanz T., Sion E. M., Tweedy R. W., 1994, ApJ, 425, L105
Holberg J. B., Barstow M. A., Bruhweiler F. C., Collins J., 1996, AJ, 111, 2361
Holberg J. B., Barstow M. A., Lanz T., Hubeny I., 1997, ApJ, 484, 871
Holberg J. B., Barstow M. A., Sion E. M., 1998, ApJS, 119, 207
Hubeny I., 1988, Comput. Phys. Commun., 52, 103
Hubeny I., Lanz T., 1995, ApJ, 439, 875
Hubeny I., Hummer D., Lanz T., 1994b, A&A, 282, 151
Hubeny I., Lanz T., Jeffrey C. S., 1994a, in Jeffrey C. S., ed, Newsletter on Analysis of Astronomical Spectra No. 20, St. Andrews Univ., p. 30
Hummer D., Mihalas D., 1988, ApJ, 331, 794
Landolt A. U., 1992, AJ, 104, 340
Lanz T., Hubeny I., 2003, ApJS, 146, 417
Lehner N., Jenkins E. B., Gry C., Moos H. W., Chayer P., Lacour S., 2003, ApJ, 595, 858
Lemke M., 1997, A&AS, 122, 285
Marsh M. C. et al., 1997, MNRAS, 287, 705
Maxted P. F. L., Marsh T. R., Moran C. K. J., 2000, MNRAS, 319, 305
Oegerle W. R., Jenkins E. B., Shelton R. L., Bowen D. V., Chayer P., 2005, ApJ, 622, 377
Schatzman E. L., 1958, in White Dwarfs. North Holland Publishing Co., Amsterdam, and Interscience Publishers, New York
Schuh S., 2005, PhD thesis, Univ. Tübingen
Schuh S., Dreizler S., Wolff B., 2002, A&A, 382, 164
Sion E. M., Schaefer K. G., Bond H. E., Saffer R. A., Cheng F. H., 1998, ApJ, 496, L29
Skrutskie M. F. et al., 1997, in Garzon F., Epchtein N., Omont A., Burton B., Persi P., eds, The Impact of Large Scale Near-IR Sky Surveys. Kluwer Academic, Dordrecht, p. 25
Vauclair G., Vauclair S., Greenstein J. L., 1979, A&A, 80, 79
Vennes S., Chayer P., Thorstensen J. R., Bowyer S., Shipman H. L., 1992, ApJ, 392, 27
Vennes S., Chayer P., Hurwitz M., Bowyer S., 1996, ApJ, 468, 898
Vennes S., Thejll P. A., Galvan R. G., Dupuis J., 1997, ApJ, 480, 714
Wolff B., Kruk J. W., Koester D., Allard N. F., Ferlet R., Vidal-Madjar A., 2001, A&A, 373, 674
Zuckerman B., Koester D., Reid I. N., Hunsch M., 2003, AJ, 506, 477

This paper has been typeset from a TEX/LATEX file prepared by the author.